https://doi.org/10.5194/tc-2019-117
Preprint. Discussion started: 26 June 2019

The Cryosphere Discussions

Sea ice volume variability and water temperature in the Greenland Sea

Valeria Selyuzhenok[1,2], Igor Bashmachnikov[1,2], Robert Ricker[3], Anna Vesman[1,2,4], and Leonid Bobylev[1]

[1]Nansen International Environmental and Remote Sensing Centre, 14 Line V.O., 7, St.Petersburg, 199034, Russia
[2]the St. Petersburg State University, Department of Oceanography, 10 Line V.O, 33, St.Petersburg, 199034, Russia
[3]Alfred-Wegener-Institut, Helmholtz-Zentrum für Polar- und Meeresforschung, Klumannstr., 3d, Bremerhaven, 27570, Germany
[4]Arctic and Antarctic Research Institute, Bering str., 38, St.Petersburg, 199397, Russia

Correspondence: Valeria Selyuzhenok (valeria.selyuzhenok@niersc.spb.ru)

Abstract. This study explores a link between the long-term variations in the integral sea ice volume (SIV) in the Greenland Sea and oceanic processes. Using Pan-Arctic Ice Ocean Modelling and Assimilation System (PIOMAS, 1979-2016), we show that the negative tendencies in SIV go in parallel with the increasing ice flux through the Fram Strait. The overall SIV loss in the Greenland Sea comprises 113 km^3 per decade, while the total SIV import through the Fram strait is increasing by 115 km^3 per decade. An analysis of the ocean temperature and the mixed layer depth (MLD) in the marginal sea ice zone (MIZ), based on ARMOR data-set (1993-2016), revealed doubling of the amount of the upper ocean heat content available for the ice melt in the MIZ. This increase over the 24-year period can solely explain the SIV loss in the Greenland Sea, even when accounting for the increasing SIV flux from the Arctic. The increase in the ocean heat content is found to be linked to an increase in the temperature of the Atlantic water in the Nordic seas, following an increase of ocean heat flux form the subtropical North Atlantic. We argue that the predominantly positive North Atlantic Oscillation (NAO) index during the four recent decades, together with the intensification of the deep convection in the Greenland Sea, are responsible for the overall intensification of the circulation in the Nordic seas, which explains the observed long-term variations of the SIV.

1 Introduction

The Greenland Sea is one of the key regions of deep ocean convection, an inherent part of the Atlantic Meridional Overturning Circulation (AMOC). The 2/3 of the deep AMOC water is formed in this region (Rhein et al., 2011; Buckley and Marshall, 2016). In turn, the intensity of convection is governed by buoyancy (heat and freshwater) fluxes at the ocean-atmosphere boundary, as well as oceanic buoyancy advection to the sea. The freshwater is thought to play the principal role in long-term buoyancy balance of the upper Greenland Sea (Meincke et al., 1992; Alekseev et al., 2001a). The positive local precipitation-evaporation exchange accounts for only 15% of the freshwater balance in the Nordic Seas. Approximately half of the fresh

https://doi.org/10.5194/tc-2019-117
Preprint. Discussion started: 26 June 2019

water anomaly in the Norwegian-Greenland region originates from the freshwater flux through the Fram Strait, which is formed by freshening of the upper ocean due to sea-ice melt in the Arctic basin and by solid ice transport (Serreze et al., 2006; Peterson et al., 2006; Glessmer et al., 2014).

The sea ice conditions in the Greenland Sea are defined by sea-ice import through the Fram Strait and by local ice formation and melt. The Fram Strait sea ice flux is primarily controlled by variations in the sea ice drift, which, in turn, are driven by the large-atmospheric circulation patterns (Vinje and Finnekåsa, 1986; Kwok et al., 2004; Ricker et al., 2018). Most of the variability of the atmospheric circulation and drift patterns is captured by the phase of the Arctic Oscillation (AO) or of its regional counterpart – the North Atlantic Oscillation (NAO) (Marshall et al., 2001). The positive AO (or NAO) phase intensifies northern winds that drives more intensive ice transport through the Fram Strait (Kwok et al., 2004). When excluding extreme negative NAO events, the correlation coefficient between NAO and sea ice area flux through the Fram Strait (over 24 years of satellite observations) reaches 0.6 Kwok et al. (2004), while that with the sea ice volume flux vary from 0.4 (over 9 years of mooring observations, 1991-1998; Kwok et al. (2004)) to 0.7 (over 7 years of CryoSat-2 satellite observations, 2010-2017; Ricker et al. (2018)). It is also argued that the interannual variations of the sea ice flux through the Fram Strait is even stronger linked to the Arctic Dipole pattern, that explains a higher fraction of the observed interannual variations in the sea-ice area flux than either the AO or the NAO (Wu et al., 2006).

The sea ice production in the Greenland Sea primarily takes place between 71-75 °N, where the highest interannual variations of sea ice area is observed (Germe et al., 2011). In the region, the Odden sea ice tongue is occasionally formed, an ice pattern extending westwards from the east Greenland shelf northwest of Jan Mayen (Wadhams et al., 1996; Comiso et al., 2001). The regression of the first empirical orthogonal function (EOF) of the sea ice extent to sea-level pressure shows a weak inverse relation with the NAO-like pattern with correlation coefficient -0.4. Further regression analysis suggests that decrease of the intensity of the northerly winds favours a larger area of the Odden sea ice tongue (Shuchman et al., 1998; Germe et al., 2011). The Odden tongue area also strongly negatively correlates with the air temperature (-0.7) over Jan Mayen and with the local sea surface temperature (-0.9) (Comiso et al., 2001). Having stronger correlations with water temperature, the negative correlation of the sea ice area with the air temperature might be an artifact, as both are oppositely affected by the oceanic heat release to the atmosphere (Germe et al., 2011).

The ocean clearly plays an important role in the sea ice melt in the region. In particular, it is speculated that the oceanic convection in the region favours a more intensive warm water flux from the south, affecting the air temperature and the sea ice extent (Visbeck et al., 1995). However, presently there is a lack of investigation linking oceanic processes with the sea ice variability in the Greenland Sea (Comiso et al., 2001; Kern et al., 2010).

Both sea ice flux through the Fram Strait and local sea ice processes in the Greenland Sea reveal changes over the recent decades. An increase of the sea ice area flux through the Fram Strait since 1979 was reported by Kwok et al. (2004); Smedsrud et al. (2017). Shorter time series of ice volume flux through the Fram Strait showed no significant changes (Kwok et al., 2004; Spreen et al., 2009; Ricker et al., 2018). At the same time, since 2000s, a reduction in winter sea ice area has been detected in the Greenland Sea (in particular in the Oddin ice tongue) from passive microwave observations (Rogers and Hung, 2008; Kern et al., 2010; Germe et al., 2011).

https://doi.org/10.5194/tc-2019-117
Preprint. Discussion started: 26 June 2019

In this paper we further explore a link between sea ice variability in the Greenland Sea and oceanic processes. The first objective is to estimate the sea ice mass balance in the Greenland Sea from local sea ice formation/melt and from sea ice advection in/out of the sea. We extend this analysis back to 1979 using the PIOMAS sea ice volume data. Further, we link the detected variations to heat flux of the Atlantic water into the region with the West Spitsbergen current (WSC).

2 Data

2.1 PIOMAS sea ice volume

PIOMAS (Pan-Arctic Ice Ocean Modeling and Assimilation System) is a coupled sea ice-ocean model developed to simulate Arctic sea ice volume. It assimilates NSIDC (National Snow and Ice Data Center) near-real time sea ice concentration, NCEP (National Centers for Environmental Prediction)/NCAR (National Center for Atmospheric Research) atmospheric parameters and the sea-surface temperature in the ice-free areas (Zhang and Rothrock, 2003).The PIOMAS provides monthly effective sea ice thickness (mean sea ice thickness over a grid cell) on a curvilinear model grid from 1978. A comparison of PIOMAS effective sea ice thickness with in situ, submarine and ICESat satellite (Ice, Cloud, and land Elevation Satellite) data, mainly covering the western Arctic, showed that the PIOMAS uncertainty for monthly mean effective sea ice thickness does not exceed 0.78 m (Schweiger et al., 2011). Although, the model tends to overestimate the thickness of the thin ice and underestimate the thickness of the thick ice, the spatial patterns of PIOMAS ice thickness agrees well with those, derived from in situ and satellite data.

Since PIOMAS performance has not been accessed south of the Fram Strait, the first part of this study is devoted to cross-validation of the PIOMAS sea ice thickness in the Greenland Sea with satellite data, as well as of the PIOMAS sea ice volume flux through the Fram Strait with satellite and upward-looking sonar (ULS) observations (Sect. 4.1 and 4.2). PIOMAS data was further used to derive time series of mean annual (September-August), mean winter (October-April) and mean summer (May-September) sea ice volume in the Greenland Sea for 1979 – 2016. The grid cell sea ice volume was computed as a product of PIOMAS effective ice thickness and the grid cell area.

2.2 AWI Cryosat-2 sea ice thickness

In the Greenland Sea PIOMAS effective sea ice thickness was cross-validated against sea ice thickness from Cryosat-2 satellite data-set (CS2 version 1.2, Grosfeld et al. (2016)). The CS2 data-set provide monthly average sea ice thickness with 25x25 km spatial resolution from 2010 to 2017. Due to limitations of ice thickness retrieval from satellite altimetry, CS2 data-set used was limited only to the cold season (October-April). The sea ice concentration data, provided along with CS2 thicknesses, was used to derive the effective sea ice thickness for the comparison with the PIOMAS data:

$$HIE_i = HI_i * SIC_i \tag{1}$$

where HI – CS2 sea ice thickness in the *i*-th grid cell, SIC - sea ice concentration in the same cell.

https://doi.org/10.5194/tc-2019-117
Preprint. Discussion started: 26 June 2019

2.3 ARMOR data-set

The long-term time series of water temperature at different depth levels and the mixed layer depth (MLD) were derived from ARMOR data-set (http://marine.copernicus.eu/, 1993-2015). The data-set combines in situ temperature and salinity profiles with satellite observations and is constructed as the following. First, based on a joint analysis of the variations of satellite-derived anomalies (sea-surface temperature and sea-level from satellite altimetry) and of in situ thermohaline characteristics at different depth, linear multiple regressions are obtained. The regressions allow extrapolating satellite data from the sea-surface to standard oceanographic levels in a regular mesh of 1/4° x 1/4 °, constructing the so-called "synthetic" vertical temperature and salinity profiles. The final monthly mean 3D temperature/salinity distributions are obtained through optimal interpolation of all observed in situ for this month together with the derived “synthetic” profiles, taken with different weights (Guinehut et al., 2012). Use of satellite information provides a more precise and detailed picture of spatial and temporal variability of the thermohaline characteristics than from interpolation of in situ profiles alone (as, for example, it is done in the World Ocean Atlas data-set). The computed vertical density profiles and the altimetry sea-surface currents were further used in ARMOR data-set for deriving current velocities at various depth levels (Mulet et al., 2012).

2.4 Water temperature of the West Spitsbergen current

Water temperatures were collected from the “Climatological Atlas of the Nordic Seas and Northern North Atlantic” (Korablev et al., 2007). The data-base merges together data from ICES (International Counsel for Exploration of the Sea) and IMR (Institute of the Marine Research) data, data from a number of international projects (ESOP, VEINS, TRACTOR, CONVECTION, etc.), as well as from Soviet Union cruises in the study region. The temperature time series, used in this paper, were obtained in the core of the WSC at 78°N (west of East-Fjord). The data were sampled in a quire irregular manner, with a particular low sampling frequency in winter. The data-gaps were filled by kriging with the 30-km window. The interannual variations used in this study were averaged from June to September – the months the most densely covered with data.

3 Methods

3.1 Fram Strait and Denmark Strait sea ice volume flux from PIOMAS

The sea ice volume flux through the Fram Strait was calculated as a product of monthly average sea ice thickness, area of the grid cell and the sea ice drift velocity (Ricker et al., 2018). Note, that the PIOMAS sea ice thickness represents the mean thickness over a grid cell, called effective sea ice thickness (with zero sea ice thickness for the open water). The gate was selected as a combination of a meridional section (82°N and 12°W - 20°E) and a zonal section (20°E and 80.5°N - 82°N), as suggested by Krumpen et al. 2016. (Fig. 1a). The location of the meridional gate at 82 °N was chosen to reduce biases and errors in sea ice drift that become larger with increasing velocities south of the gate (Sumata et al., 2014, 2015). The meridional and zonal sea ice volume flux, Q_v and Q_u correspondingly, were computed as:

https://doi.org/10.5194/tc-2019-117
Preprint. Discussion started: 26 June 2019

$$Q_v = l/cos(\lambda) * H * (D_x sin(\lambda) - D_y cos(\lambda)) \quad (2)$$

$$Q_u = l/cos(\lambda) * H * (D_x cos(\lambda) - D_y sin(\lambda)) \quad (3)$$

where l = 25 km is the distance between 2 data-points, H is the PIOMAS sea ice thickness and D_x, D_y represents sea ice drift velocity in *x* and *y* directions, respectively, and λ is the longitude of the respective grid cell. The total ice volume flux through the Fram Strait (QF, positive – into the Greenland Sea) was obtained as a sum of the meridional and zonal fluxes along the gate:

$$QF = Q_u + Q_v \quad (4)$$

The total ice volume flux through the Fram Strait was derived for the period from 1979 to 2017 for each months. A similar methodology was used to assess the sea ice volume flux though the Denmark strait along the meridional section (66°N and 25°W – 36°E) In order to access the data quality, the resultant ice volume fluxes though the Fram Strait gate at 82°N were cross-validated against available satellite-based estimates in the Fram Strait from Kwok et al. (2004); Spreen et al. (2009); Ricker et al. (2018). The gate and the methodology used here was adopted from Ricker et al. (2018), while in other two studies somewhat different methodologies and gates locations (Fig. 1a) were used. Each of the studies also is based on different data-set of sea ice concentration (SIC), thickness (SIT) and drift (SID) (Tab.1).

3.2 Greenland Sea sea ice mass balance

In order to analyse the sea ice volume lost or formed due to thermodynamically within the Greenland Sea, we calculated the sea ice mass balance (MB) in the Greenland Sea. It was derived for each month from 1979 to 2016 as:

$$MB = (QF_m - QD_m) - (V_m - V_{(m-1)}) \quad (5)$$

where V_m and $V_(m-1)$ are regional sea ice volume of the current *m*-th and previous *(m-1)*-th months, QF_m and QD_m are Fram Strait and Denmark Strait sea ice volume flux of the current *m*-th month. Therefore, positive MB values correspond to sea ice melt and negative values correspond to sea ice formation within the Greenland Sea. The mass balance shows month-to-month increase or loss in sea ice volume within the Greenland Sea due to sea ice formation or melt. The monthly MB values were averaged over annual, winter and summer periods. Note, that due to averaging positive annual values corresponding to sea ice volume loss (Fig.4) can occur due to both an increase in sea ice melt and a decrease in sea ice formation.

3.3 Mixed layer depth (MLD) and marginal ice zone (MIZ) ocean temperature

The MLD was derived using vertical profiles from ARMOR data-set by the method of Dukhovskoy (Bashmachnikov et al., 2018, 2019). The method is similar to that used by Pickart et al. (2002), but is applied to the vertical profiles of density gradients. Before processing, the potential density profiles were filtered to remove the small-scale noise. The gravitationally

https://doi.org/10.5194/tc-2019-117
Preprint. Discussion started: 26 June 2019

unstable segments were artificially mixed to neutral stratification. The MLD is defined as the depth where the vertical density gradient exceeds its two local standard deviations within a 50-m window, centred at the tested point. The visual control shows that the results are mostly similar to the widely used methods by de Boyer de Boyer Montégut et al. (2004) and Kara et al. (2003), except for the weakly stratified areas, where the Dukhovskoy's method defines the MLD with higher accuracy. The marginal ice zone was defined as an area enclosed between the 500-m isobath (marking the shelf break) and the mean winter location of the sea ice edge (Fig. 1). The sea ice edge was defined as the 15% mean winter NSIDC sea ice concentration for 1979-2016.

3.4 Oceanic horizontal heat flux

The ARMOR data was used to derive a time series of oceanic heat flux into the Nordic Seas. Total oceanic heat flux through the transect (Q) is calculated by integrating the heat flux values in the grid points:

$$Q_i = \rho * c_p * (T_i - T_{ref}) V_w d_x d_z \quad (6)$$

where ρ =1030 kg m^{-3} is the mean sea water density; c_p = 4200 J kg^{-1} $^\circ$ C^{-1} is specific heat of sea water; T_i is sea water temperature in an *i*-th grid cell T_{ref} =-1.8°C is the "reference temperature", V is current speed perpendicular to the transect, d_x is the distance between the vertical profiles along the transect, d_z is the thickness of the water layer for the processed depth level.

4 Results

4.1 Assessment of PIOMAS-derived ice volume flux through the Fram Strait and sea ice volume in the Greenland Sea

In order to assess the quality of the PIOMAS data in the region, PIOMAS monthly effective sea ice thickness in the Greenland Sea was compared to those derived using the CS2 data-set (Fig. 2). In general, PIOMAS underestimate effective sea ice thickness compared to the CS2 (Fig. 1b). The mean difference between PIOMAS and CS2 of a grid cell values is - 0.70 m. There are only two locations where PIOMAS shows thicker ice compared to the CS2 – north of the Spitsbergen and along the sea ice edge. The highest absolute differences between the data sets are attributed to the areas along the Greenland coast (dark blue) and north of the Spitsbergen (dark red) (Fig. 1b). The monthly scatter plots (Fig. 2a-g) show that PIOMAS tend to overestimates thin sea ice and underestimate thick sea ice thickness, which is in agreement with the tendency reported for the central Arctic Schweiger et al. (2011). This results in moderate correlations between the two data sets (0.63 < r < 0.77) for all winter months. The major discrepancies correspond to sea ice of 3 m and higher thickness, which form "tails" to the lower right corner of the scatter plots (Fig. 2 a-g).

PIOMAS sea ice volume flux through the Fram Strait (October to April) was cross-compared with the satellite-derived and ULS-based ice thickness data (see Tab.1). The analysis shows that ice volume fluxes in PIOMAS are in good agreement with the estimates from other data sets (Fig. 3, Tab. 2). The correlation coefficients between the three data sets and the PIOMAS all are over 0.6. The highest correlation over 0.8 with Ricker et al. (2018) data can be explained by using identical gates and

https://doi.org/10.5194/tc-2019-117
Preprint. Discussion started: 26 June 2019

methodology for estimating ice volume fluxes (Fig. 1a). However, other statistical criteria (bias, relative percentage difference (RPD), root mean square error (RMSE), Tab.2) indicate somewhat stronger mismatch between the PIOMAS and Ricker et al. (2018) ice volume fluxes compared to those between PIOMAS and Kwok et al. (2004) or Spreen et al. (2009). The possible sources of these discrepancies are discussed in Sec. 5. Overall, PIOMAS shows lower ice volume fluxes compared to the satellite- and the ULS-based estimates (Fig. 3c). The interannual variations in the PIOMAS monthly and total winter flux agree well with other data-sets (Fig. 3a; Tab. 2) until 2014, after which PIOMAS fluxes start decreasing, contrary to the results by Ricker et al. (2018). At intra-annual time scales all three data-sets show similar patterns with the minimum flux in October and maximum flux in March (Fig. 3b). Overall, moderate to high correlation between the data-sets, low relative variance and low bias (Tab. 2) suggest that PIOMAS provides a realistic estimate of seasonal and interannual variations of the winter sea ice flux through the Fram Strait. Figures 2h and 3c suggest that PIOMAS correctly captures year-to-year variations of the mean effective sea ice thickness in the Greenland Sea and Fram Strait sea ice volume flux. This justifies using PIOMAS for analysing interannual variations of the integral sea ice volume over the Greenland Sea.

4.2 Interannual variations of sea ice flux through the Fram Strait and sea ice volume in the Greenland Sea

The sea ice volumes in the Greenland Sea, derived from PIOMAS, revealed statistically significant negative trends in winter, summer and annual values (Fig. 4a, Tab. 3). The strongest negative trend of 84.8 km ^{3} per decade or 13.5% of long-term annual mean volume is observed in winter, while for summer months, the trend comprises 58.2 km^3 per decade or 9.3% of long-term annual mean volume. The sea ice volume in the Greenland Sea shows an overall reduction by 72.4 km^3 or 11.5% of its long-term mean per decade. The reduction of the sea ice volume in the Greenland Sea unexpectedly goes along with an increase in the monthly ice volume flux through the Fram Strait by 9.6 km^3 per decade or 8.8% of its long-term mean (significant at 90% confidence level). Thus, the total increase in the sea ice volume imported to the Greenland Sea though the Fram Strait comprises 112.8 km^3 per decade, which accounts for 17.8% of the Greenland Sea annual mean sea ice volume. The sea ice volume flux through the Denmark Strait comprises for about 2% (Fig. 2) of that through the Fram Strait and shows no significant tendency. This flux has no significantly effect on the sea ice balance of the sea. A balance between SIV import/export to the Greenland Sea though the straits and regional changes in SIV shows the volume of ice formed or lost due to thermodynamic processes within the region (Sec. 3.2). The sea ice mass balance in the Greenland Sea expressed in SIV loss is shown in Fig. 4b. The SIV loss shows positive statistically significant trends in annual and summer values, while winter trend shows low statistical significance (Tab. 3). Overall, the monthly Greenland Sea SIV loss increases by 9.4 km^3 per decade (Fig. 4, Tab. 3).

4.3 Interannual variations of water temperature and MLD in the MIZ of the Greenland Sea

In order to find the reason for the opposite trends of SIV in the Greenland Sea and ice volume flux though the Fram Strait, we investigate water temperature in the study region (Sec. 2.3, 3.3, 3.4). A relatively warm Atlantic water is observed in the East Greenland Current (EGC), off the Greenland shelf break, below a thin upper mixed layer dominated by the cold Polar water. The Atlantic water is regularly brought to the ocean surface by vertical mixing, which intensifies in winter (Håvik et al.,

https://doi.org/10.5194/tc-2019-117
Preprint. Discussion started: 26 June 2019

2017). The presence of the Atlantic water is observed in climatology as water temperature (and salinity) in the EGC increasing southeastwards and downwards from about 0 °C at the sea-surface to 2-4°C at 500 m. In the 24-year means, the northern temperature maximum (Fig. 5a) results from recirculation of Atlantic water of the WSC in the southern Fram Strait, while the southern maximum is due to the northwards heat flux with the West Islandic Current (WIC) through the Denmark Strait (Ypma et al., 2019). The latter is a northern branch of the Irminger Current. In the annual means, the water temperature, averaged over upper 50-m layer of the MIZ, has maximum of 2°C in September and decreases to 0.1-0.2°C in March-April. Always above the seawater freezing temperatures, the ocean melts the sea ice in the MIZ all the year-round.

Figure 5a shows interannual variations of November 2 °C sea water isotherm (averaged over the 200-m layer). From 1990s to 2000s the isotherm approaches the shelf break. The largest westwards propagation is observed in the WSC recirculation area (76-78°N) and northwest of Yan Mayen (70-73°N). The linear temperature trends (Fig. 5b) confirm the overall warming in the western and southern parts of the MIZ, linked to a stronger warming of the Norwegian Atlantic Front Current (NwAFC), of its extension – the WSC, as well as of the WIC. The mean upper ocean salinity (Fig. 5c) and its tendencies (Fig. 4d) confirm the increasing presence of the Atlantic water in the upper 50-m layer in the MIZ. Averaged over the upper 200-m, the typical depth of the winter mixed layer (not shown), the patterns of the mean distribution and of (a somewhat weaker) tendencies in temperature and salinity closely repeat those in Figure 5.

Interannual variations of water characteristics, averaged over the upper 200-m and over the MIZ area, are shown in Figure 6. From 1993, an overall year mean increase of temperature in the MIZ is observed, suggesting an increasing intensity of the sea ice melt. The temperature increases during all seasons, but the strongest increase is detected in autumn (by 0.5 and 0.6°C over the 24 years). The winter convection efficiently uplifts heat to the sea surface. The heat is released to the atmosphere and goes to the sea ice melt, decreasing the interannual trends to insignificant (see Tab.3). Therefore, from 1993, we also observe an increase of the water temperature difference from September to March (Fig. 6a), e.g., in the upper 200-m layer the heat accumulated in summer is mostly released during winter.

Not only the autumn temperature increases in the MIZ, the zonal thermal gradient across the MIZ nearly doubles from 1993 in annual mean (Fig. 6b), and even stronger (2.5 times) increases in winter. This goes together with a decrease by half of the annual mean distance of the 3°C isotherm to the shelf break (Fig. 6d): from 120 km in 1993 to 50 km in 2016 (see also Fig.5a). The direct result of this effect is a faster melt of the sea ice episodically advected from the MIZ eastwards by EGC filaments and mesoscale eddies (Kwok, 2000; von Appen et al., 2018). These processes can transport sea ice dozens of kilometers eastward (von Appen et al., 2018). The most favourable conditions for the eddy formation observed for the northern winds (Bondevik, 2011). This increases the ice melt, however, a few episodic observations of the ice dynamics in the MIZ do not presently allow quantifying the importance of this effect. The 24-year mean winter mixed layer depth (MLD) in the MIZ off the Greenland shelf vary from 120 m to 250 m with the mean value around 150 m, as derived from ARMOR data-set. Averaged over the MIZ, MLD increases from the mean value of 130 m in 1993 to around 180 m in 2016 (Fig. 6c). Since the winter mixing does not reach the lower limit of the warm Atlantic water at 500-700 m, the deeper the mixing, the more heat is uplifted towards the sea-surface, melting the ice in the MIZ. The increase of MLD results from a higher upper ocean density due to increasing salinity of the Atlantic water, tempered by the increasing temperature (Fig. 5b,d). Given the increase in

https://doi.org/10.5194/tc-2019-117
Preprint. Discussion started: 26 June 2019

ocean temperature in the upper 200-m layer in the MIZ from 1.3°C in September 1993 to 1.8°C in September 2016 together with an increase in the mean winter MLD from 130 m in 1993 to 180 m in 2016, we can make a rough estimate of the increase (over the 24 years) in the heat released by winter MLD in the MIZ:

$$dQ = dQ_{2016} - dQ_{1993} = c_p * \rho * (2.0 * 180 - 1.3 * 130) * MIZarea \quad (7)$$

where c_p = 4200 J $^{\circ}C^{-1}$ kg^{-1}, ρ = 1030 kg m^{-3} , the MIZ area is estimated as 2.3 10^{11} m^2, which is about 20% of the area of the Greenland Sea. The computations show an additional heat release of 2 10^{20} J, if, following the observed water temperature seasonal cycle, we assume that all the heat from the growing winter MLD is released at the sea-surface. If all this heat would go to melt ice in the MIZ, we get an increase in the SIV loss during winter by:

$$dV = dq/(L * \rho_L) \sim 600km^3 \quad (8)$$

where the specific heat of ice fusion L=3.3 10^5 J kg^{-1} and the ice density of ρ_L = 920 kg m^{-3} (Petrich and Eicken, 2010). This far exceeds the the observed sea ice volume loss in the region (SIV loss monthly winter trend * 12 month * 24 years = 340 km^{-3}) of ice needed to fuse. Certainly, not all heat, released by the upper ocean goes to the ice melt, a unknown fraction of heat is transferred to the atmosphere through open water and leads or advected away from the MIZ area by ocean currents and eddies. However, the estimates above suggest that solely the on-going warming of the Greenland Sea water can result in the reduction of SIV in the Greenland Sea.

5 Discussion

5.1 PIOMAS-derived trends

The revealed regional trends in sea ice volume rely on the PIOMAS model data. A comparison of interannual variations of PIOMAS regional sea ice thickness and the volume flux through the Fram Strait showed that PIOMAS estimates are in agreement with the satellite-based data during the recent decades. However, the PIOMAS systematic overestimation of thin ice and underestimation of thick ice thickness, reported for the central Arctic, affects the multiyear volume trend (Schweiger et al. 2011). The authors conclude that the PIOMAS-based volume trend is lower that the actual one. Given that similar systematic errors in effective sea ice thickness are found for the Greenland Sea (Fig. 2), it is likely that the derived Greenland Sea sea ice volume trend is underestimated. The PIOMAS Fram Strait sea ice volume flux appear to be lower compared to know from literature fluxes (Fig. 3). The main sources of relative errors between the Fram Strait volume flux estimates can be related to the different choice of methodologies, sets of the data and gates used to derive volume fluxes (Tab.1, Fig.1). Lower PIOMAS-based flux can be attributed to the discussed above general PIOMAS tendency to underestimate sea ice thickness. Fig. 2i shows that for the entire meridional 82 °N gate, the PIOMAS effective sea ice thickness is lower compared to the CS-2. In addition, the NSIDC sea ice drift shows lower speed compared to the OSI SAF drift used in Ricker et al. (2018). A combination of lower drift speed with thinner ice thickness might be the reason of the largest offset (Tab.2, Fig. 3) between the PIOMAS-based Fram Strait fluxes and those derived in Ricker et al. (2018).

https://doi.org/10.5194/tc-2019-117
Preprint. Discussion started: 26 June 2019

The revealed decrease in the sea ice volume in the Greenland Sea goes in parallel with an increase in the ice volume inflow through the Fram Strait. As the ice volume flux through the Denmark Strait does not show any significant change, this indicates a simultaneous intensification of the processes of ice melt and reduction in sea ice formation in the sea. The latter is supported by the highest negative trends in the sea ice area (SIA) (Fig. 1, expressed in SIC trend) in the area of the Odden tongue between 73 and 77°N, which is mostly formed locally thermodynamically, at cold air temperatures (Shuchman et al., 1998; Comiso et al., 2001; Rogers and Hung, 2008). The intensification of in the sea ice melt is discussed in the following section. The interannual variations SIA were previously related with the corresponding variations in the air temperature (Comiso et al., 2001).In this study we argue that at least the overall SIV loss from 1993 to 2016 is governed by the ocean.

5.2 Link to the variability of ocean temperature and atmospheric forcing

The surplus of the amount of the heat, released by the ocean at end of the study period, is almost twice of necessary for bringing up the observed SIV loss, even when accounting for the detected increase in the SIV transport through the Fram Strait. Heat loss to the atmosphere and the neighbouring ocean areas should uptake the rest of the heat. In particular, the observed increase of ocean temperature over the Greenland Sea (Fig. 5b) may be a reason for a corresponding increase in the air temperature, used for explaining negative trends in the SIA (Comiso et al., 2001).

The observed trends are due to both, the increase in temperature of the Atlantic water in the MIZ, as well as an increase in winter MLD in the area, brining more Atlantic water to the surface. A significant vertical extent of the warm subsurface Atlantic water later, going down to 500-700 m depth (Håvik et al., 2017), results in a higher ocean heat release for a stronger mixing for the observed MLD in the MIZ. A similar mechanism was suggested for in the Nansen basin of the Arctic Ocean, where an enhanced vertical mixing through the pycnocline is thought to decrease the SIA in the basin (Ivanov and Repina, 2018).

In turn, the subsurface Atlantic water in the EGC is fed by the recirculation of the surface water of the West Spitsbergen Current, an extension of the Norwegian Atlantic Front Current (NwAFC) and the Norwegian Atlantic Slope Current (NwASC). The recirculation is through to be mostly driven by eddies (Boyd and D'Asaro, 1994; Nilsen et al., 2006; Hattermann et al., 2016). The detected inconsistency is due to local peculiarities in interannual variations in the vertical mixing intensity, in local ocean-atmosphere exchange and a the degree of delution of the advected Atlantic water with the Polar water with its own interannual variability. All the processes intensify during highly dynamic winter conditions. Nevertheless, interannual correlation of the summer upper ocean water temperature (0-200 m), spatially averaged over the MIZ area, with that in the upper WSC is 0.8-0.9. Further south, correlation of interannual variations of the MIZ temperature with that of the NwAFC (NwASC) or with the heat flux across the Svinoy section are low. Besides differences in local forcing, regional atmospheric forcing over the northwestern Barents Sea, regulates the interannual variations of the heat re-distribution between the WSC and the Barents Sea (Lien et al., 2013), further decreasing the correlations.

Nevertheless, in a long run (during four recent decades), temperature at the WSC, the NwAFC, NwSFC and the heat flux across Svinoy section all show positive trends (Fig. 4, 5). This is confirmed by in a number of studies (Alekseev et al., 2001b; Piechura and Walczowski, 2009; Beszczynska-Möller et al., 2012).

https://doi.org/10.5194/tc-2019-117
Preprint. Discussion started: 26 June 2019

Several studies show that during the positive NAO phase, the intensity of oceanic heat flux to the Nordic seas increases by 50%, and the NwASC intensifies along the Scandinavian coast (Skagseth et al., 2004; Raj et al., 2018). On the other hand, the positive NAO phase drives a higher ice drift through the Fram Strait, proved to be the main driver for interannual variations of SIF to the Greenland Sea (Ricker et al., 2018). It is also noted that the positive NAO phase increases of the intensity of the EGC (Blindheim et al., 2000; Kwok, 2000). Finally, the link between the Atlantic water transport by the WSC and the cyclonic circulation in the Greenland Sea, related to NAO phase, is obtained from observations and numerical models (Walczowski, 2010; Chatterjee et al., 2018).

Summing up the results above, the positive phase of NAO intensifies the whole current system of the Nordic Seas, simultaneously intensifying sea ice flux through the Fram Strat and Atlantic water flux to the Nordic seas. The simultaneous long-term (1974-1997) intensification of the Atlantic water inflow in the Nordic Seas through the Faroe-Shetland ridge, and of eastwards advection Polar Water to the southwestern Norwegian Sea, as a response to NAO forcing has been noted in (Blindheim et al., 2000). This supports our conclusions. From the beginning of 1970s the winter NAO index is growing. From 1979 to 2016 it is mostly positive (Fig. 7), although an overall winter trend can be separated into an increase from 1979 to 1994, a rapid drop from 1995 to 1996 and an increase from 1996 to 2016. The NAO index drop 1995-1996 is observed as a drop in SIV loss and decrease in the WSC water temperature (Fig. 4b,e), and can be related to the minimum heat flux through the Svinoy section in 1994 (Fig. 4f). The time needed for water properties to propagate from Svinoy to the Fram Strait with the NwAC is of order of 1.5-2 years (Walczowski, 2010).

Summer NAO index does not govern the interannual variations of the atmospheric system, as well as in the oceanic ones (circulation in the Nordic seas intensifies in winter and is thought to bring more Atlantic Water to the recirculation region compared to than in summer). Consistent with other studies of seasonal interannual variations of current intensity in the region, our results suggest that these are winter variations of the Atlantic water transport that bring up the interannual variations of the subsurface water temperature in the MIZ of the Greenland Sea. The decreasing summer NAO index from 1979, may be responsible for a somewhat stronger tendency in the SIV decrease in winter, compared to summer (Fig. 4a,b).

In spite of the stronger ice melt, the upper ocean salinity in MIZ, as well as along the main currents in the Greenland Sea, increases during recent decades (Fig. 5d). We relate salinification in the MIZ area of the upper Greenland Sea to a stronger flux of the Atlantic water and more intensive winter mixing. These effects override the additional freshwater input from the ice melt. Oppositely, during freshening of the upper Greenland Sea, the Great salinity anomaly 1966-1972, more ice is observed in the MIZ region – Odden ice tongue was pronounced (Rogers and Hung, 2008). This confirms the reverse relation between the sea ice content and the MIZ salinity in the Greenland Sea and their dependence on interannual variations of the intensity of the Atlantic Water advection.

Another, possibly not independent mechanism is linked to the intensity of the deep convection in the Greenland Sea (Fig. 7). Governed by thermohaline characteristics of the upper Greenland Sea, the ice extent and the intensity of ocean-atmosphere heat and freshwater exchange (Marshall and Schott, 1999; Moore et al., 2015), the more intense convection lowers the sea-level in the Greenland Sea (Gelderloos et al., 2013; Bashmachnikov et al., 2019), thus increasing the cyclonic circulation in the region. This effect works together with NAO forcing. Deep convection in the Greenland Sea shows a consistent increase

https://doi.org/10.5194/tc-2019-117
Preprint. Discussion started: 26 June 2019

from about 1000 m in the beginning of 1990s to about 1500-2000 m during 2008-2010, after which a certain tendency to decrease is noted (Bashmachnikov et al., 2019). The on-going increase in salinity of the upper Greenland Sea (Fig. 5d) during the recent decades favours the deeper convection. Satellite altimetry data show that, during the same period, the area-mean cyclonic vorticity over the Nordic Seas has grown by about 10%. The circulation increase is also consistent with the detected intensification of the AMOC after its minimum in 1980s (Rahmstorf et al., 2015).

6 Conclusions

Using PIOMAS sea ice volume data we derived trends in the mean annual, winter and summer sea ice volume (SIV) in the Greenland Sea and the sea ice volume flux (SIF) through the Fram Strait for 1979 to 2016. Taking into account the SIV inflow and outflow though the Fram and Denmark Straits, the thermodynamic SIV loss within the Greenland Sea was derived. It shows an increase in monthly SIV loss by 9.4 km^3 per decade. From 1979 to 2016 the overall SIV loss comprises $\sim$ 270 km^3, in spite of an increase ice SIF by $\sim$ 280 km^3 during the same time period.

Our analysis of the upper ocean water properties in the marginal sea ice zone of the EGC, shows a notable increase of the Atlantic Water temperature below the pycnocline, as well as of winter mixed layer depth from 1993 to 2016. These changes result in a higher sea-surface heat release, providing twice the value of additional heat needed for bringing up the observed SIV loss. Therefore, the long-term variations of the heat flux entering the Nordic Seas, advected northwards with the NwAC as the Atlantic Water and, further on, with the WSC into the MIZ, are found to govern the corresponding long-term SIV variations in the Greenland Sea. The analysis of marginal sea ice zone (MIZ) ocean parameters showed an increase in mixed layer depth (MID) and its temperature from 1993 to 2016. The estimated amount of additional oceanic heat released from 1993 to 2016 surplus the amount of necessary for bringing up the observed SIV loss. Therefore, we state that the Atlantic Water advection into the MIZ largely contributes to the SIV loss.

The long-term variations of the Atlantic water transport all the way through the Froe-Shetland ridge, with the WSC and to the MIZ zone. Interannual variations between the parameters, though, do not have high correlations, governed by variations in the local forcing.

We also showed that the simultaneous tendencies in the long-term increase of SIF and of the Atlantic water transport are both linked to a higher intensity of atmospheric circulation during the positive NAO phase, and, possibly, to the intensity of deep convection. Not being independent, both mechanisms finally lead to a decrease of SIV in the western Greenland Sea.

Acknowledgements. The research was supported by RSF, project No. 17-17-01151.

https://doi.org/10.5194/tc-2019-117
Preprint. Discussion started: 26 June 2019

References

Alekseev, G., Johannessen, O., and Kovalevskii, D.: Development of convective motions under the effect of local perturbations of sea-surface density, Izvestiya Atmospheric and Oceanic Physics, 37, 341–350, 2001a.

Alekseev, G. V., Johannessen, O. M., Korablev, A. A., Ivanov, V. V., and Kovalevsky, D. V.: Interannual variability in water masses in the Greenland Sea and adjacent areas, Polar Research, 20, 201–208, https://doi.org/https://doi.org/10.1038/ncomms2505, 2001b.

Bashmachnikov, I., Fedorov, A., Vesman, A., Belonenko, T., Koldunov, A., and Dukhovskoy, D.: The thermohaline convection in the subpolar seas of the North Atlantic from satellite and in situ observations. Part 1: localization of the deep convection sites, Russian/Sovremennye problemy distantsionnogo zondirovaniya Zemli iz kosmosa, 15, 184–194, https://doi.org/DOI:10.21046/2070-7401-2018-15-7-184-194, 2018.

Bashmachnikov, I., Fedorov, A., Vesman, A., Belonenko, T., and Dukhovskoy, D.: The thermohaline convection in the subpolar seas of the North Atlantic from satellite and in situ observations. Part 2: ndices of intensity of deep convection, Russian/Sovremennye problemy distantsionnogo zondirovaniya Zemli iz kosmosa, 16, 191–201, https://doi.org/DOI: 10.21046/2070-7401-2019-16-1-191-201, 2019.

Beszczynska-Möller, A., Fahrbach, E., Schauer, U., and Hansen, E.: Variability in Atlantic water temperature and transport at the entrance to the Arctic Ocean, 1997–2010, ICES Journal of Marine Science, 69, 852–863, 2012.

Blindheim, J., Borovkov, V., Hansen, B., Malmberg, S.-A., Turrell, W., and Østerhus, S.: Upper layer cooling and freshening in the Norwegian Sea in relation to atmospheric forcing, Deep Sea Research Part I: Oceanographic Research Papers, 47, 655–680, https://doi.org/-, 2000.

Bondevik, E.: Studies of Eddies in the Marginal Ice Zone Along the East Greenland Current Using Spaceborne Synthetic Aperture Radar (SAR), Master's thesis, The University of Bergen, 2011.

Boyd, T. J. and D'Asaro, E. A.: Cooling of the West Spitsbergen Current: wintertime observations west of Svalbard, Journal of Geophysical Research: Oceans, 99, 22 597–22 618, 1994.

Buckley, M. W. and Marshall, J.: Observations, inferences, and mechanisms of the Atlantic Meridional Overturning Circulation: A review, Reviews of Geophysics, 54, 5–63, 2016.

Chatterjee, S., Raj, R. P., Bertino, L., Skagseth, Ø., Ravichandran, M., and Johannessen, O. M.: Role of Greenland Sea Gyre Circulation on Atlantic Water Temperature Variability in the Fram Strait, Geophysical Research Letters, 45, 8399–8406, https://doi.org/https://doi.org/10.1029/2018GL079174, 2018.

Comiso, J. C., Wadhams, P., Pedersen, L. T., and Gersten, R. A.: Seasonal and interannual variability of the Odden ice tongue and a study of environmental effects, Journal of Geophysical Research: Oceans, 106, 9093–9116, 2001.

de Boyer Montégut, C., Madec, G., Fischer, A. S., Lazar, A., and Iudicone, D.: Mixed layer depth over the global ocean: An examination of profile data and a profile-based climatology, Journal of Geophysical Research: Oceans, 109, 2004.

Gelderloos, R., Katsman, C., and Våge, K.: Detecting Labrador sea water formation from space, Journal of Geophysical Research: Oceans, 118, 2074–2086, https://doi.org/-, 2013.

Germe, A., Houssais, M.-N., Herbaut, C., and Cassou, C.: Greenland Sea sea ice variability over 1979–2007 and its link to the surface atmosphere, Journal of Geophysical Research: Oceans, 116, 2011.

Glessmer, M. S., Eldevik, T., Våge, K., Nilsen, J. E. Ø., and Behrens, E.: Atlantic origin of observed and modelled freshwater anomalies in the Nordic Seas, Nature Geoscience, 7, 801, 2014.

Grosfeld, K., Treffeisen, R., Asseng, J., Bartsch, A., Bräuer, B., Fritzsch, B., Gerdes, R., Hendricks, S., Hiller, W., Heygster, G., et al.: Online sea-ice knowledge and data platform< www. meereisportal. de, Polarforschung, 85, 143–155, 2016.

https://doi.org/10.5194/tc-2019-117
Preprint. Discussion started: 26 June 2019

Guinehut, S., Dhomps, A.-L., Larnicol, G., and Traon, P.-Y. L.: High resolution 3-D temperature and salinity fields derived from in situ and satellite observations, Ocean Science, 8, 845–857, https://doi.org/-, 2012.

Hattermann, T., Isachsen, P. E., von Appen, W.-J., Albretsen, J., and Sundfjord, A.: Eddy-driven recirculation of Atlantic water in Fram Strait, Geophysical Research Letters, 43, 3406–3414, https://doi.org/doi: 10.1002/2016GL068323, 2016.

Håvik, L., Pickart, R. S., Våge, K., Torres, D., Thurnherr, A. M., Beszczynska-Möller, A., Walczowski, W., and von Appen, W.-J.: Evolution of the East Greenland current from Fram Strait to Denmark strait: synoptic measurements from summer 2012, Journal of Geophysical Research: Oceans, 122, 1974–1994, 2017.

Ivanov, V. and Repina, I.: The Effect of Seasonal Variability on the State of the Arctic Sea Ice Cover, Izvestiya rossiyskoy akademii nauk. Fizika atmosfery i okeana, 54, 73–82, https://doi.org/DOI: 10.7868/S0003351518010087, 2018.

Kara, A. B., Rochford, P. A., and Hurlburt, H. E.: Mixed layer depth variability over the global ocean, Journal of Geophysical Research: Oceans, 108, 2003.

Kern, S., Kaleschke, L., and Spreen, G.: Climatology of the Nordic (Irminger, Greenland, Barents, Kara and White/Pechora) Seas ice cover based on 85 GHz satellite microwave radiometry: 1992–2008, Tellus A, 62, 411–434, 2010.

Korablev, A., Pnyushkov, A., and Smirnov, A.: Compiling of the oceanographic database for climate monitoring in the Nordic Seas, Russian/Trudy AARI, 447, 85–108, 2007.

Kwok, R.: Recent changes in Arctic Ocean sea ice motion associated with the North Atlantic Oscillation, Geophysical Research Letters, 27, 775–778, 2000.

Kwok, R. and Rothrock, D. A.: Variability of Fram Strait ice flux and North Atlantic Oscillation, Journal of Geophysical Research: Oceans, 104, 5177–5189, https://doi.org/10.1029/1998JC900103, https://agupubs.onlinelibrary.wiley.com/doi/abs/10.1029/1998JC900103, 1999.

Kwok, R., Cunningham, G., and Pang, S.: Fram Strait sea ice outflow, Journal of Geophysical Research: Oceans, 109, 2004.

Lien, V. S., Vikebø, F. B., and Skagseth, Ø.: One mechanism contributing to co-variability of the Atlantic inflow branches to the Arctic, Nature Communications, 4, 1488, https://doi.org/-, 2013.

Marshall, J. and Schott, F.: Open-ocean convection: Observations, theory, and models, Reviews of Geophysics, 37, 1–64, https://doi.org/-, 1999.

Marshall, J., Kushnir, Y., Battisti, D., Chang, P., Czaja, A., Dickson, R., Hurrell, J., McCartney, M., Saravanan, R., and Visbeck, M.: North Atlantic climate variability: phenomena, impacts and mechanisms, International journal of climatology, 21, 1863–1898, 2001.

Meincke, J., Jonsson, S., and Swift, J. H.: Variability of convective conditions in the Greenland Sea, in: ICES Mar. Sci. Symp, vol. 195, pp. 32–39, 1992.

Moore, G. W. K., Våge, K., Pickart, R. S., and Renfrew, I. A.: Decreasing intensity of open-ocean convection in the Greenland and Iceland seas, Nature Climate Change, 5, 877, https://doi.org/https://doi.org/10.1038/nclimate2688, 2015.

Mulet, S., Rio, M.-H., Mignot, A., Guinehut, S., and Morrow, R.: A new estimate of the global 3D geostrophic ocean circulation based on satellite data and in-situ measurements, Deep Sea Research Part II: Topical Studies in Oceanography, 77, 70–81, 2012.

Nilsen, F., Gjevik, B., and Schauer, U.: Cooling of the West Spitsbergen Current: Isopycnal diffusion by topographic vorticity waves, Journal of Geophysical Research: Oceans, 111, 2006.

Peterson, B. J., McClelland, J., Curry, R., Holmes, R. M., Walsh, J. E., and Aagaard, K.: Trajectory shifts in the Arctic and subarctic freshwater cycle, Science, 313, 1061–1066, 2006.

Petrich, C. and Eicken, H.: Growth, structure and properties of sea ice, Sea ice, 2, 23–77, 2010.

https://doi.org/10.5194/tc-2019-117
Preprint. Discussion started: 26 June 2019

Pickart, R. S., Torres, D. J., and Clarke, R. A.: Hydrography of the Labrador Sea during active convection, Journal of Physical Oceanography, 32, 428–457, 2002.

Piechura, J. and Walczowski, W.: Warming of the West Spitsbergen Current and sea ice north of Svalbard, Oceanologia, 51, 147–164, https://doi.org/https://doi.org/10.5697/oc.51-2.147, 2009.

Rahmstorf, S., Box, J. E., Feulner, G., Mann, M. E., Robinson, A., Rutherford, S., and Schaffernicht, E. J.: Exceptional twentieth-century slowdown in Atlantic Ocean overturning circulation, Nature climate change, 5, 475, https://doi.org/https://doi.org/10.1038/nclimate2554, 2015.

Raj, R. P., Nilsen, J. Ø., Johannessen, J., Furevik, T., Andersen, O., and Bertino, L.: Quantifying Atlantic Water transport to the Nordic Seas by remote sensing, Remote Sensing of Environment, 216, 758–769, https://doi.org/https://doi.org/10.1016/j.rse.2018.04.055, 2018.

Rhein, M., Kieke, D., Hüttl-Kabus, S., Roessler, A., Mertens, C., Meissner, R., Klein, B., Böning, C. W., and Yashayaev, I.: Deep water formation, the subpolar gyre, and the meridional overturning circulation in the subpolar North Atlantic, Deep Sea Research Part II: Topical Studies in Oceanography, 58, 1819–1832, https://doi.org/https://doi.org/10.1016/j.dsr2.2010.10.061, 2011.

Ricker, R., Girard-Ardhuin, F., Krumpen, T., and Lique, C.: Satellite-derived sea ice export and its impact on Arctic ice mass balance, The Cryosphere, 12, 3017–3032, 2018.

Rogers, J. C. and Hung, M.-P.: The Odden ice feature of the Greenland Sea and its association with atmospheric pressure, wind, and surface flux variability from reanalyses, Geophysical Research Letters, 35, 2008.

Schweiger, A., Lindsay, R., Zhang, J., Steele, M., Stern, H., and Kwok, R.: Uncertainty in modeled Arctic sea ice volume, Journal of Geophysical Research: Oceans, 116, 2011.

Serreze, M. C., Barrett, A. P., Slater, A. G., Woodgate, R. A., Aagaard, K., Lammers, R. B., Steele, M., Moritz, R., Meredith, M., and Lee, C. M.: The large-scale freshwater cycle of the Arctic, Journal of Geophysical Research: Oceans, 111, 2006.

Shuchman, R. A., Josberger, E. G., Russel, C. A., Fischer, K. W., Johannessen, O. M., Johannessen, J., and Gloersen, P.: Greenland Sea Odden sea ice feature: Intra-annual and interannual variability, Journal of Geophysical Research: Oceans, 103, 12 709–12 724, 1998.

Skagseth, Ø., Orvik, K. A., and Furevik, T.: Coherent variability of the Norwegian Atlantic Slope Current derived from TOPEX/ERS altimeter data, Geophysical Research Letters, 31, https://doi.org/https://doi.org/10.1029/2004GL020057, 2004.

Smedsrud, L. H., Halvorsen, M. H., Stroeve, J. C., Zhang, R., and Kloster, K.: Fram Strait sea ice export variability and September Arctic sea ice extent over the last 80 years, The Cryosphere, 11, 65–79, 2017.

Spreen, G., Kern, S., Stammer, D., and Hansen, E.: Fram Strait sea ice volume export estimated between 2003 and 2008 from satellite data, Geophysical Research Letters, 36, 2009.

Sumata, H., Lavergne, T., Girard-Ardhuin, F., Kimura, N., Tschudi, M. A., Kauker, F., Karcher, M., and Gerdes, R.: An intercomparison of A rctic ice drift products to deduce uncertainty estimates, Journal of Geophysical Research: Oceans, 119, 4887–4921, 2014.

Sumata, H., Gerdes, R., Kauker, F., and Karcher, M.: Empirical error functions for monthly mean Arctic sea-ice drift, Journal of Geophysical Research: Oceans, 120, 7450–7475, 2015.

Vinje, T. and Finnekåsa, Ø.: The ice transport through the Fram Strait, 1986.

Visbeck, M., Fischer, J., and Schott, F.: Preconditioning the Greenland Sea for deep convection: Ice formation and ice drift, Journal of Geophysical Research: Oceans, 100, 18 489–18 502, 1995.

von Appen, W.-J., Wekerle, C., Hehemann, L., Schourup-Kristensen, V., Konrad, C., and Iversen, M. H.: Observations of a Submesoscale Cyclonic Filament in the Marginal Ice Zone, Geophysical Research Letters, 45, 6141–6149, https://doi.org/10.1029/2018GL077897, https://agupubs.onlinelibrary.wiley.com/doi/abs/10.1029/2018GL077897, 2018.

https://doi.org/10.5194/tc-2019-117
Preprint. Discussion started: 26 June 2019

Wadhams, P., Comiso, J., Prussen, E., Wells, S., Brandon, M., Aldworth, E., Viehoff, T., Allegrino, R., and Crane, D.: The development of the Odden ice tongue in the Greenland Sea during winter 1993 from remote sensing and field observations, Journal of Geophysical Research: Oceans, 101, 18 213–18 235, 1996.

Walczowski, W.: Atlantic Water in the Nordic Seas–properties, variability, climatic significance, OCEANOLOGIA, 52, 325–327, https://doi.org/doi: 10.1007/978-3-319-01279-7, 2010.

Wu, B., Wang, J., and Walsh, J. E.: Dipole anomaly in the winter Arctic atmosphere and its association with sea ice motion, Journal of Climate, 19, 210–225, 2006.

Ypma, S., Brüggemann, N., Georgiou, S., Spence, P., Dijkstra, H., Pietrzak, J., and Katsman, C.: Pathways and watermass transformation of Atlantic Water entering the Nordic Seas through Denmark Strait in two high resolution ocean models, Deep Sea Research Part I: Oceanographic Research Papers, https://doi.org/https://doi.org/10.1016/j.dsr.2019.02.002, 2019.

Zhang, J. and Rothrock, D.: Modeling global sea ice with a thickness and enthalpy distribution model in generalized curvilinear coordinates, Monthly Weather Review, 131, 845–861, 2003.

https://doi.org/10.5194/tc-2019-117
Preprint. Discussion started: 26 June 2019

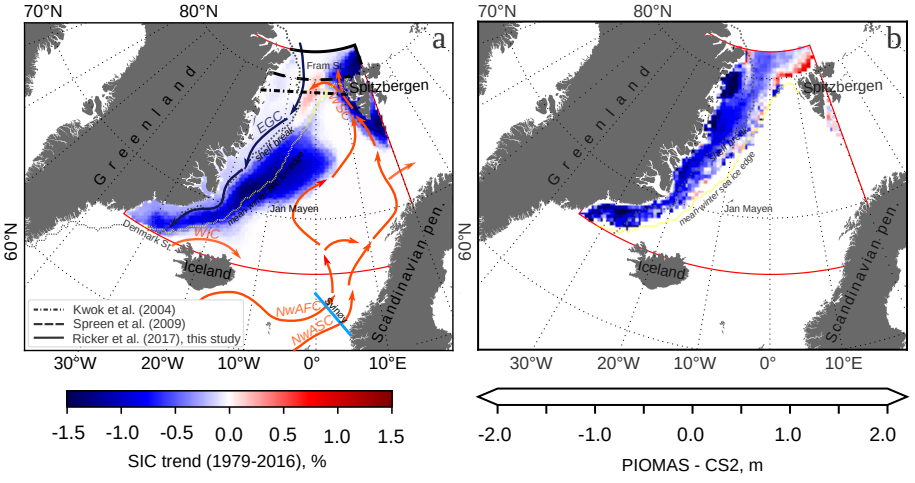

Figure 1. The study region is marked with the red box: a - linear trends in the mean September-April NSIDC sea ice concentration (SIC) over the period 1979-2016. The black lines show gates used for estimation of the sea ice volume flux through the Fram Strait. Mean winter sea ice edge is shown in dash yellow, the shelfbreak (500-m isobash) is shown in dash grey. EGC is the East Greenland Current, WIC – the West Islandic Current, NwAFC – the Norwegian Atlantic Front Current,NwASC – the Norwegian Atlantic Slope Current, WSC – the West Spitsbergen Current; b - difference between mean PIOMAS and CS2 effective ice thickness (m).

https://doi.org/10.5194/tc-2019-117
Preprint. Discussion started: 26 June 2019

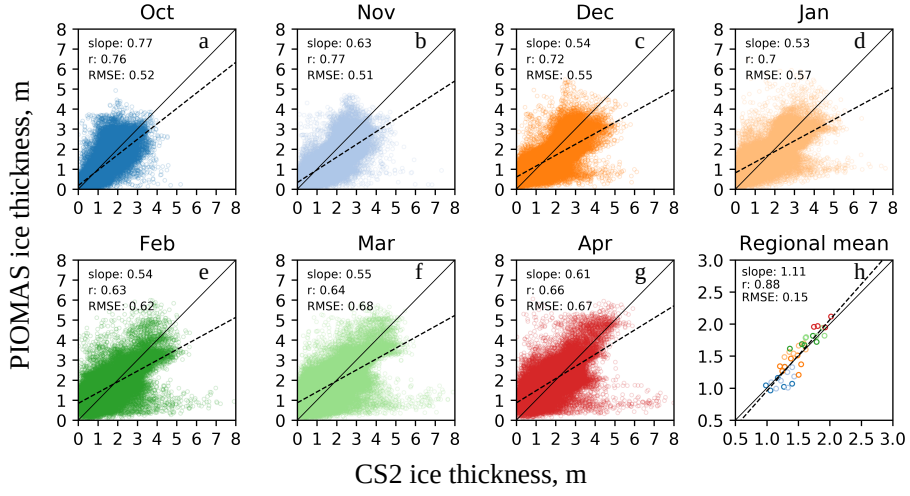

Figure 2. Scatter plots of PIOMAS and CS2 monthly effective sea ice thickness (m) in the Greenland Sea, October-April 2010-2016: (a-g) - each point corresponds to one grid-cell sea ice thickness; (h) area-mean monthly sea ice thickness over the ice covered area of the Greenland Sea; (i) – difference between mean PIOMAS and CS2 effective ice thickness (m). The color of the points in corresponds to the color of the months from October to April (2010-2016) at panels a-g. The dashed lines show the linear regression fit and the solid lines are 45° angles. The correlation coefficients (r) and the slope of the linear regressions are given in the upper left corner.

https://doi.org/10.5194/tc-2019-117
Preprint. Discussion started: 26 June 2019

The Cryosphere
Discussions
Open Access
EGU

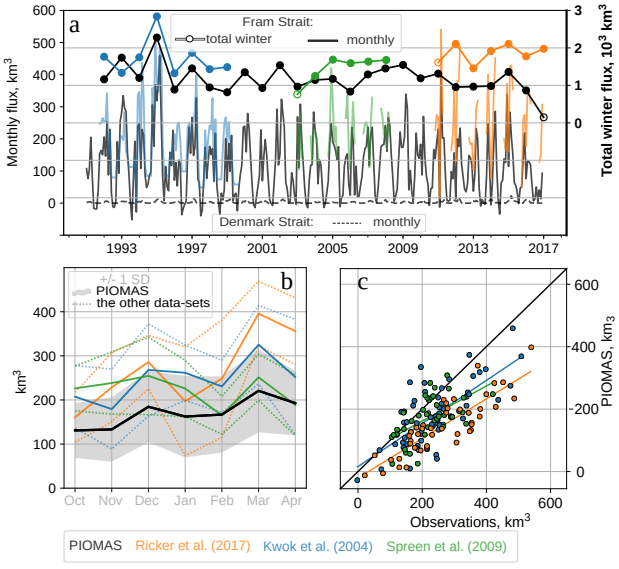

Figure 3. Sea ice volume fluxes (km^3): a - time series of PIOMAS and satellite-based monthly sea ice volume fluxes (km3) through the Fram and the Denmark Straits, 1991-2017 (note that the mean fluxes are referenced to the right scale). Empty circles indicate seasons with an incomplete winter cycle: b - winter intra-annual cycle through the Fram Strait, averaged over the period of the observations and over 1991-2016 for PIOMAS data-set. The dash lines (satellite estimates) and the gray background color (PIOMAS) correspond to one standard deviation interval from the mean; c - scatter diagram of monthly mean PIOMAS volume fluxes through the Fram Strait versus monthly mean observations.

https://doi.org/10.5194/tc-2019-117
Preprint. Discussion started: 26 June 2019

The Cryosphere
Discussions
Open Access
EGU

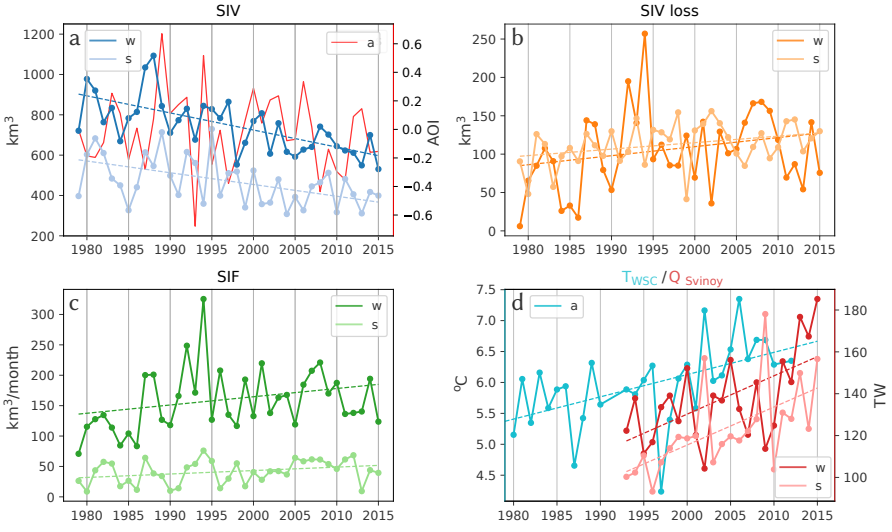

Figure 4. Time series of winter means (December-April) and summer means (May-November) ice-ocean-atmosphere characteristics in the Greenland Sea: (a) PIOMAS sea ice volume (SIV, km^3) and summer AO index (AOI), (b) PIOMAS sea ice volume loss (SIV loss, km^3), (d) annual means of water temperature in the West Spitsbergen Current (TWSC, °C/year) and ocean heat flux (TW) through Svinoy section (see Fig. 1).

https://doi.org/10.5194/tc-2019-117
Preprint. Discussion started: 26 June 2019

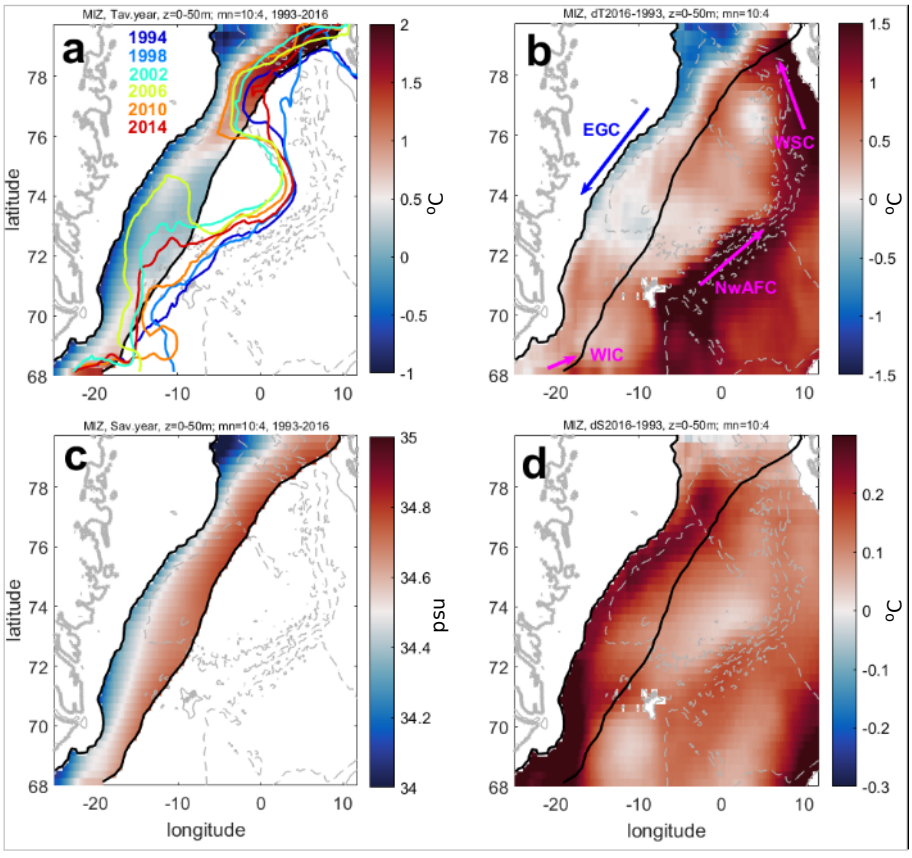

Figure 5. Marginal sea ice zone (enclosed in black lines) and themohaline water properties averaged in the upper 50-m layer during cold season (October-April). a - time-mean (1993-2016) temperature (°C) in MIZ and location of 2°C isotherm in November for selected years; b - linear change in temperature (°C) in the upper 50 m-layer from 1993 to 2016; c - time-mean (1993-2016) salinity in MIZ; d) linear change in salinity in the upper 50-m layer from 1993 to 2016. In plate (b) EGC is the East Greenland Current, WIC – the West Islandic Current, NwAFC – the Norwegian Atlantic Front Current, WSC – the West Spitsbergen Current.

https://doi.org/10.5194/tc-2019-117
Preprint. Discussion started: 26 June 2019

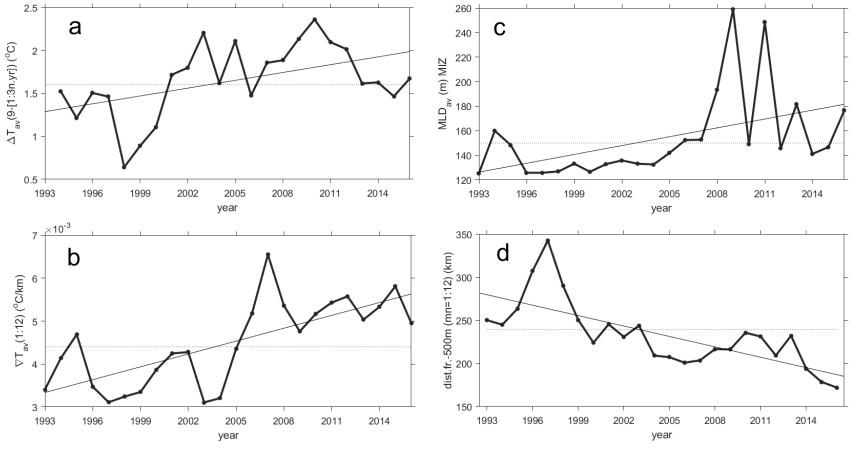

Figure 6. Interannual variations of water properties, averaged over the 200-m layer and the MIZ area. (a) Temperature drop (°C) from maximum in September to minimum in March next year; (b) annual mean temperature gradient across the MIZ (°C km⁻1); (c) the mixed layer depth (m), averaged over the cold season); (d) annual mean distance of the 3°C isotherm from the shelf break (km).

https://doi.org/10.5194/tc-2019-117
Preprint. Discussion started: 26 June 2019

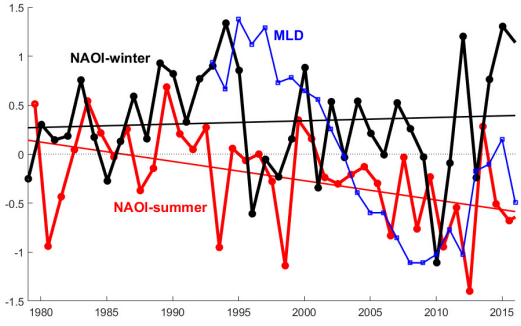

Figure 7. Cold season NAOI (black, November-April) and warm season NAOI (red, May-October) with linear trends; normalized maximum MLD in the Greenland Sea derived from ARMOR data-set (Bashmachnikov et al. (2019) for details)

https://doi.org/10.5194/tc-2019-117
Preprint. Discussion started: 26 June 2019

Table 1. The list of data sources used for estimates of sea ice volume flux through the Fram Strait: sea ice concentrations (SIC), sea ice thicknesses (SIT), sea ice drift velocities (SID) and the time periods of the estimates.

Study	SIC	SIT	SID	Period
Kwok et al. (2004)	ULS moorings	ULS moorings	Kwok and Rothrock (1999)	1991-2002
Spreen et al. (2009)	ASI AMSR-E	ICESat	IFREMER	2003-2008
Ricker et al. (2018)	OSI SAF SIC + sea ice type product	AWI Cryosat-2	OSI SAF	2010-2017
this study	-	PIOMAS	NSIDC Pathfinder v2	1979-2017

Table 2. Statistics of monthly PIOMAS versus satellite-based estimates of the sea ice volume fluxes through the Fram Strait: Pearson correlation coefficient (cor. coef), variance relative to PIOMAS (var. rel.), bias, relative percentage difference (RPD), root mean square error (RMSE).

Study	cor.coef.	mean slope	var. rel.,%	bias	RPD,%	RMSE,km^3
Kwok et al. (2004)	0.70	0.71	98	47	66	75
Spreen et al. (2009)	0.60	0.61	97	33	45	56
Ricker et al. (2018)	0.84	0.66	162	107	88	108

var. rel.,% = $(100\% * var_{obs})/var_{PIOMAS}$
bias = $obs. - PIOMAS$

https://doi.org/10.5194/tc-2019-117
Preprint. Discussion started: 26 June 2019

Table 3. Trends in monthly mean characteristics in the Greenland Sea calculated over annual (September-August), winter (October-April) and summer (March-September) periods: sea ice volume (SIV, km^3/year), sea ice volume loss (SIV loss, km^3/year), sea ice flux though the Fram Strait (SIF Fram, km^3/year), water temperature in MIZ (Tw, °C/year) and in the West Spitsbergen Current (TWSC, °C/year), heat flux across the Svinoy section (Q_{Svinoy}, TW/year).

parameter	season	trend	r^2	STD	p-value
SIV, km^3/year	annual	-7.24 (-1.15%)	0.42	1.48	<0.01
	winter	-8.48 (-1.35%)	0.44	1.66	<0.01
	summer	-5.82 (-0.93%)	0.26	1.72	<0.01
SIV loss, km^3/year	annual	0.94 (0.88%)	0.09	0.52	0.08
	winter	1.18 (1.10%)	0.06	0.83	0.17
	summer	0.84 (0.79%)	0.10	0.45	0.07
SIF Fram, km^3/month/year	annual	0.96 (0.88%)	0.09	0.53	0.08
	winter	1.36 (1.25%)	0.08	0.82	0.10
	summer	0.56 (0.52%)	0.09	0.32	0.08
Tw, °C/year	annual	0.015 (1.50%)	0.23	0.007	0.04
	winter	0.008 (0.01%)	0.05	0.007	0.29
	summer	0.026 (3.00%)	0.29	0.008	<0.01
Q_{Svinoy}, TW/year	annual	1.84 (1.39%)	0.48	0.41	<0.01
	winter	1.83 (1.38%)	0.35	0.54	<0.01
	summer	1.82 (1.37%)	0.36	0.53	<0.01
T_{WSC},°C/year	annual	0.036 (0.60%)	0.30	0.30	<0.01